

Advanced thermal manikin with neuro-fuzzy control

Mircea Dan¹, Paul Danca², Ioan Ursu¹, Ilinca Nastase²,

¹INCAS - National Institute for Aerospace Research "Elie Carafoli"
B-dul Iuliu Maniu 220, Bucharest 061136, Romania
E-mail: ursu.ioan@incas.ro

² CAMBI, Technical University of Civil Engineering in Bucharest, Building Services Department, 66 Avenue Pache Protopesc; 020396, Bucharest, Romania

Abstract. *This paper is presenting one among the five prototypes of thermal manikins conceived at the Building Services Faculty (Thermal-Hydraulic Systems Laboratory) at the Technical University of Civil Engineering of Bucharest and developed by the National Institute of Aerospace Research Elie Carafoli in the framework of the project EQUATOR. This particular prototype has an advanced anatomic shape, with 79 independent active zones, temperature sensors and its own in-house software for data acquisition and control of the zone's surface temperature. The paper is presenting the all stages needed for the development of an advanced thermal manikin with neuro-fuzzy control for research purposes. All composing parts of the manikin and the validation strategy were presented.*

Key words: advanced thermal manikin, thermal confort, neuro-fuzzy control

1. Introduction

Thermal comfort is a complicated concept defined by a plurality of subjective parameters. A thermal manikin is a human model designed for testing of thermal environments without some inconveniences inherent in human subject testing. Thermal manikins are mainly used in automotive, indoor environment, outdoor environment, military and clothing research. Thermal manikins have a long time history, being used for more than 70 years. At the beginning they were used for testing clothing for soldiers by the US Army [1]. The shape and heating system were very simple at that stage. Nowadays the shape and complexity of the available thermal manikins raised and start to approach the complexity of the human body. The number of independently controlled zones increased from a single zone corresponding to the entire surface up to 120 individually controlled zones [2]. The material used for developing the thermal manikin have diversified, from copper to plastic and carbon fiber to skin like silicone. Most of them try to simulate the human body and the associated heat emission in the environment, while others are more or less complex measurement devices for assessing thermal environment quality by simulating the human body thermal regulatory mechanisms and measuring its heat loss towards its environment [1]. The most advanced of them can also simulate body sweating and heat exchange through evaporation [1-4]. This paper is presenting one advanced thermal

manikin with neuro-fuzzy control that was developed in the framework of the EQUATOR project [5].

Nomenclature	
θ [m]	temperature
P [W]	mean power consumption calculated using a sliding average over a preset period of time
S [m ²]	surface area of manikin's region
<i>Subscripts</i>	
ech	equivalent
reg	region

2. Manufacturing the heating part of the manikin

This particular prototype, is a female manikin, familiarly called Suzi. It has an advanced anatomic shape, with 79 independent active zones, 5 temperature sensors for each zone and its own in-house software for data acquisition and control. The thermal manikin was designed for both seated and standing postures. The size of the manikin is a standard human size with a total surface of 1.8m² (Fig. 1a). The base structure of the manikin is made of polyvinyl. The surface of the manikin has been covered with a 5mm insulation layer (Fig. 1b).

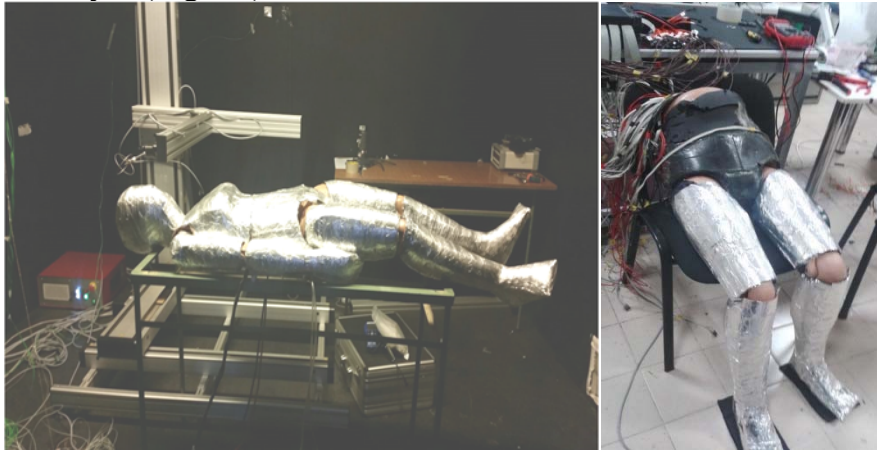


Fig.1 a) Thermal manikin simulating a patient, b) manufacturing the body parts – the black part is representing the insulation layer

The heating solution chosen for this prototype consist in using five types of elementary patches (Fig. 2a) that are combined to cover each individually controlled zone. The patches are made of a thin layer of silicone (1.5mm) that includes a heating circuit made of nickel chrome heating wire and etching foil. The heating silicone patches are presented in Fig. 2b. Several solutions of films and heating materials were tested but the heating silicone patches were found to provide the best uniformity in terms of temperature distribution. In Fig. 4 are compared the surface temperature distributions of a flexible polyamide heating film, of a silicone patch and of the human

skin of the hand. The heating film patches were placed on the insulation layer on the polyvinyl base using with double side adhesive tape. After covering a body zone the electrical connections and circuits were created. Every electrical connection was tested for leakage for safety reasons. The electrical wire was embedded inside the manikin (Fig 1b). In order to ensure that the thermal load of the film mounted over the wires is not influencing the cable stability we selected special electrical wire that works at temperatures above 7°C. During a preliminary test, without any control of the circuits, the temperature of each zone stabilized at 45°C when the room temperature was stable at 24 °C, a rather encouraging result offering a wide range to control the temperature of each zone and the possibility to simulate different cases of body heat release.

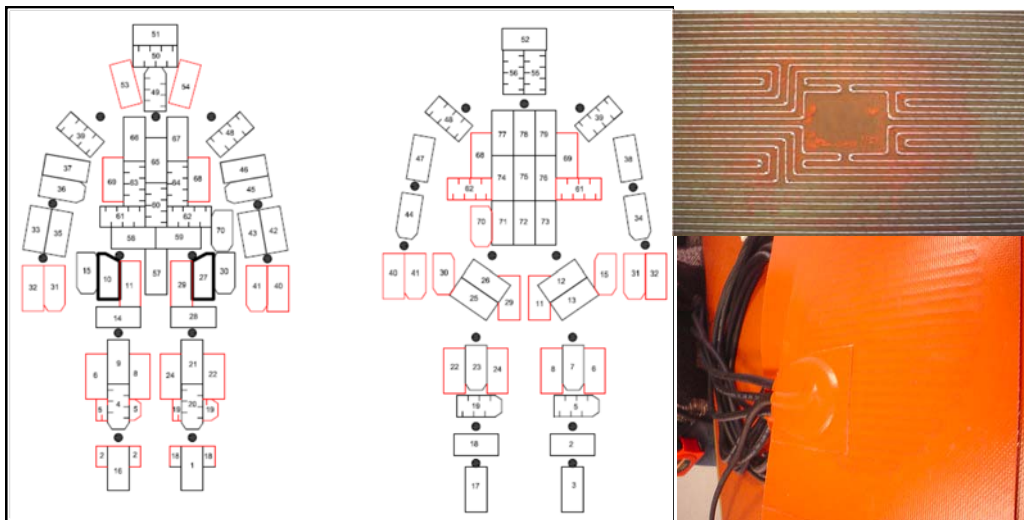


Fig.2 a) Distribution of the anatomic zones individually controlled (red patches are corresponding to the other side), b) Photographs of the heating silicon parts that are composing the zones

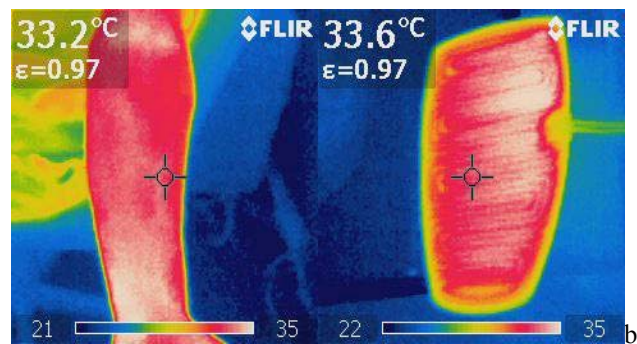


Fig. 3) Comparison between the surface temperature distribution of a silicone patch and the human skin of the hand [6].

Even if this type of heating element appeared to be the best possible solution for the current project there are still some regions where the heating circuit is not present creating zones where the temperature values are lower (i.e. the borders of each patch – see Fig. 6 b for instance). As a non-uniform temperature of the manikin surface has to be avoided [7] we decide to cover the entire manikin surface with adhesive aluminium foil to ensure enhanced conduction heat transfer. Finally, in order to facilitate further investigations with a thermal (IR) camera the entire manikin surface was covered with

a transparent adhesive film. In order to validate the heating part of the manikin prototype we performed several tests, concerning the distribution of the surface temperature of each manikin, the sensors employed for the control part, the electrical characteristics of the used components.

For the control part of the surface temperature of the manikin we choose digital sensors given the adopted strategy presented previously. The sensors are the model TSic T501 manufactured by IST. Each sensor was carefully tested. In Fig. 5 a) and b) are presented examples of response at thermal solicitations over time for eight of these sensors with and without calibration. During the calibration process we used a thermostatic water bath Lauda Eco with immersion thermostat Lauda Eco Silver (Fig. 12 c).



Fig 4. a) TSic T501 sensors used for the measurement and control part of the thermal manikin , b) thermostatic water bath Lauda Eco with immersion thermostat Lauda Eco Silver

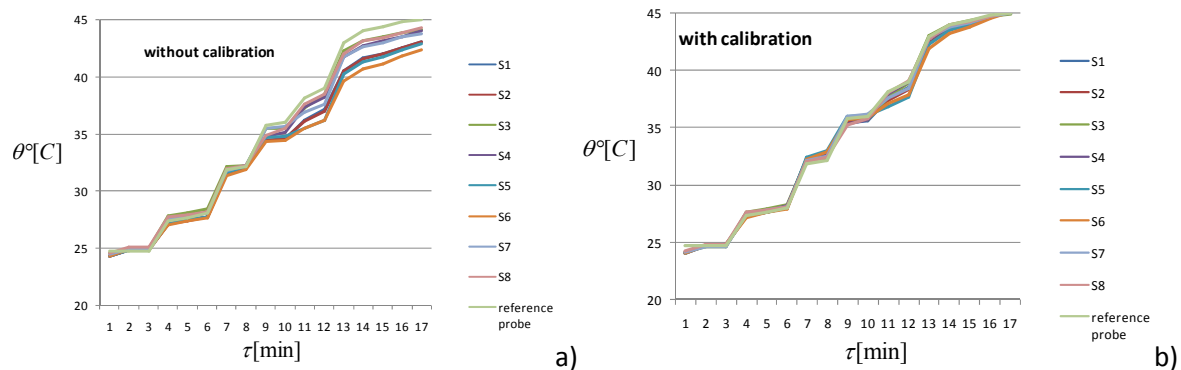


Fig 5. Response at thermal solicitations over time of TSic TO92 sensors: a) without calibration, b) with calibration

3. Architecture of the control system of the thermal manikin

The thermostatic manikin system consists of 79 patches each with a heating element (24 Ohms constant resistance) and 5 analog temperature sensors (TSic 501) mounted on each patch surface used by the control system to maintain a constant preset temperature of the manikin surface. The 395 acquisition channels are collected by the multiplexer interface (Fig. 6) to help miniaturizing of the electronic system, by reducing the space occupied by wires, thus being able to fit inside the manikin.

For the development of the system there were used two boards from National Instruments (myRIO 1900 and sbRIO 9363). Both have a unit of sequent calculus

(x86) and unit of matrix calculus. To connect the temperature sensors to the development board there was used a multiplexer interface based on HEF4067B. The control of the MOS transistors used for the execution system was achieved through an interface made of SN7407 circuits. Basic architecture of the manikin system is given in Fig. 7.

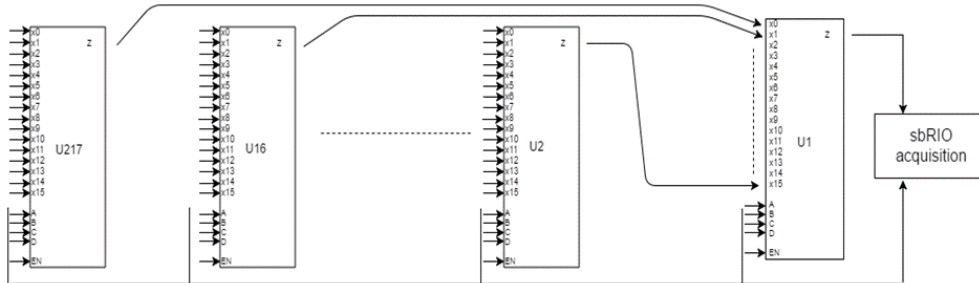


Fig 6. Multiplexer simplified circuit diagram

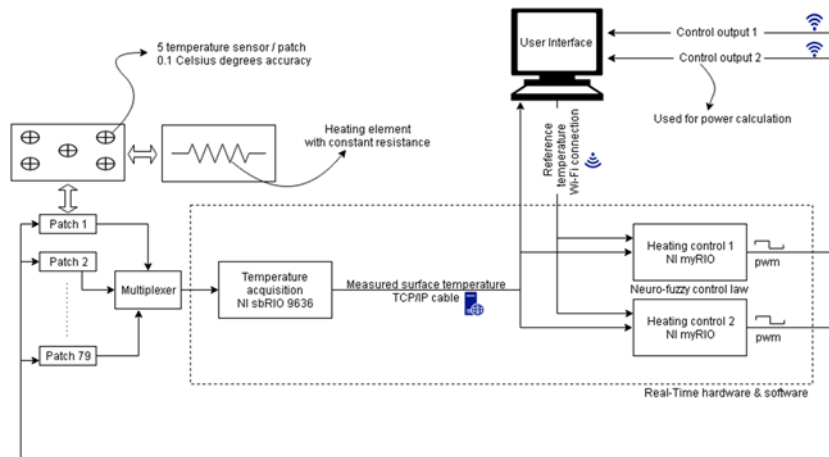


Fig. 7. Basic architecture of manikin system

The FPGA software on the sbRIO 9636 handles the acquisition of data from the multiplexer interface which, instead of requesting one input at a time, collects all the inputs and separates them by shifting the register in the temperature data memory. The software from myRIO 1900's FPGA creates the PWM pulse used to control the patch surface. Both NI boards have implemented real-time software, the acquisition device also processes the data to obtain reliable mean temperature of every patch using a fault detection and isolation algorithm, while the heating control devices, using the data processed by the acquisition board, generate robust and adequate signal using the neuro-fuzzy controller. The real-time hardware and software can run independently from the computer user interface, with the limitation of maintaining the last (or default) requested set point of temperature.

The computer software allows the user to load set points for several testing situations, change the set point on each patch independently and monitor the behavior of the temperature data and control system. The user can also view the average equivalent temperature displayed graphically on a simplified model of manikin and average power consumption.

The necessity of processing a high amount of information (395 acquisition channels, signal filtering, etc.) and generating proper signals for 79 command channels, as well as the strict timing, provided by the NI boards Real-Time processor and required for the control of electronic circuits (multiplexer and MOS driver interface), lead clearly to the conclusion that this technology is the best solution for the manikin system. The control algorithm for the command channels was converted into software for the sequent calculus unit of the NI boards.

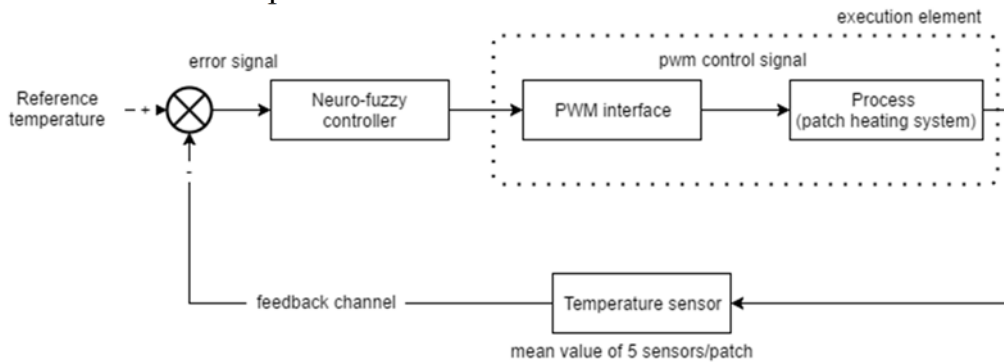


Fig 8. Control system diagram for one control channel

Block-schema for the control of one channel is shown in Fig. 8. PWM (pulse width modulation) is a well known technique to produce analog signal using digital devices that output a square signal by switching on and off the output port. By modifying the period that the signal is on and off, a voltage between 0 and 24V (the maximum voltage recommended for the patches) can be provided. Since myRIO 1900 boards can output only 3.3V in DIO (digital I/O) ports, there has been added an interface to convert 3.3V TTL signal to 5V CMOS signal needed by the transistors to open and close the 24V supply circuit according to the PWM control generated by the neuro-fuzzy controller. In fact, the salient feature of neurocontrol and fuzzy logic control, which distinguish them from the traditional control and adaptive approaches, is that they provide a model-free description of the control system. Thus, a lot of troubles relating to the robustness of the system can be surpassed. Both neural networks and fuzzy logic show great potential for controlling systems that are difficult or impossible to model using traditional techniques. The advantages of neural networks are twofold: learning ability (a neural network mimics the function of the brain) and versatile mapping capabilities from input to output (certain types of neural networks are universal approximators giving so special abilities in adaptive control and system identification). In its turn, the fuzzy set theory provides a suitable tool for both the treatment of intrinsic inexactness of the description in a dialectical context and imitation of human thinking in the process of compromise in making a decision [8], [9]. For the thermal manikin, the temperature is optimally controlled: neural network minimizes the temperature reference tracking error. For the synthesis of neuro-fuzzy control, only a measured temperature information is required, and it is not necessary to know a mathematical model of the manikin system!

4. Thermal comfort indicators

The equivalent temperature that represents an indication of thermal comfort is obtained by evaluating the power consumption of a region of the manikin. Due to the pwm control signal which commutes on and off between maximum and minimum voltage, the power consumed by the thermostatic system was calculated by creating a calibration slope between pwm duty-cycle and the power calculated as a point by point mean of a single pulse period. The voltage drop on the patch was calculated differentially by measuring with the Hantek DSO5102P oscilloscope the voltage drop on the whole circuit from which it was subtracted the voltage drop on the transistors. The current consumed by the patch was measured with TH5A current transducer.

$$\theta_{ech} = \theta_{reg} - \frac{P}{S \cdot h_{cal}} \tag{11}$$

where θ_{ech} = equivalent temperature; θ_{reg} = mean temperature of surface region calculated using a sliding average over a preset period of time; S = surface area of manikin's region; P = mean power consumption calculated using a sliding average over a preset period of time; h_{cal} = convection coefficient calculated with equation (1) at constant environment temperature (θ_{ech}) of 24 °C and manikin's surface temperature controlled at 34 °C. Experiments revealed that by modifying the environment temperature from 20 to 40°C the changes in power consumption were indistinguishable (Fig. 9).

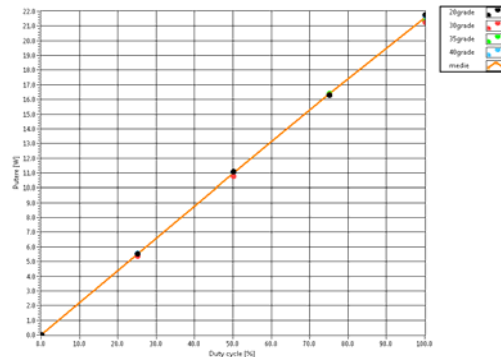


Fig 9. Power variation as function of PWM duty-cycle

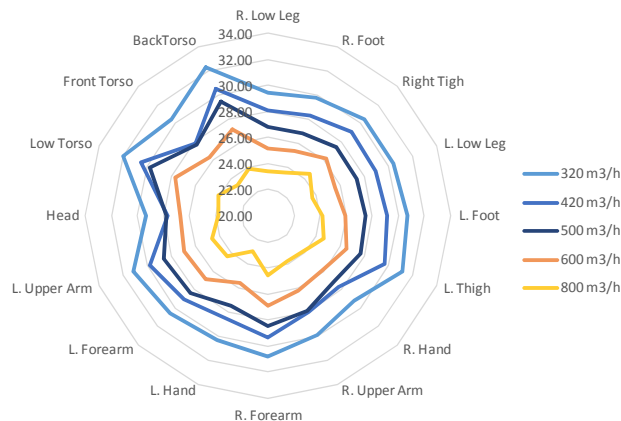


Fig. 10. Example of θ_{ech} distributions obtained from the thermal manikin data for several air flows

Compared to classical measurement systems which give the possibility of estimating the global PMV, the thermal manikin gives the advantage of assessing locally a predicted local sensation, either through the equivalent temperature either through a derived local PMV. The thermal manikin represents a worthy tool for the thermal comfort analysis in laboratory configurations and in real field case studies being a method of investigating local discomfort through the local distributions of the equivalent temperature of the segments of the manikin. This kind of representation allows, for instance, the inspection of the uniformity of an environment. In Figure 10, we show an example of equivalent temperature distributions for several air flows defined by Nilsson [10] or in the standard EN ISO 14505/2 [11] for a studied air grille for operating rooms.

6. Conclusions

This paper is presenting the all stages needed for the development of an advanced thermal manikin for research purposes. All composing parts of the manikin and the validation strategy were presented. A carefully check-up of all components was necessary and some of the tests we done were time consuming. The model is fully functional and the temperatures of each body zone can be easily modified in accordance to our needs.

Acknowledgements

This work was supported by the grants of the Romanian National Authority for Scientific Research, CNCS – UEFISCDI, project numbers: PN-II-ID-PCE-2011-3-0835 and PN-II-PT-PCCA-2011-3.2-1212”.

References

1. Holmér, I., *Thermal manikin history and applications*. European Journal of Applied Physiology, 2004. **92** p. 614-618.
2. Jambunathan, K., et al., *A review of heat transfer data for single circular jet impingement*. International Journal of Heat and Fluid Flow, 1992. **13**: p. 106-115.
3. Alahmer, A., et al., *Vehicular thermal comfort models; a comprehensive review*. Applied Thermal Engineering, 2011. **31**(6–7): p. 995-1002.
4. Sakoi, T., et al., *Thermal comfort, skin temperature distribution, and sensible heat loss distribution in the sitting posture in various asymmetric radiant fields*. Building and Environment, 2007. **42**(12): p. 3984-3999.
5. *EQUATOR: Advanced strategies for high performance indoor Environmental quality in Operating Rooms - PN-II-PT-PCCA-2011-3.2-0512*. 2012-2016, UEFISCDI.
6. Dogeanu, A., *Cercetari privind realizarea unor proceduri performante de evaluare si clasificare a microclimatului interior, Teza de doctorat*. 2015.
7. Gardon, R. and J.C. Akfirat, *The role of turbulence in determining the heat-transfer characteristics of impinging jets*. International Journal of Heat and Mass Transfer, 1965. **8**: p. 1261-1272.

8. Ursu, I., et al., *Neuro-fuzzy synthesis of flight controls electrohydraulic servo*. Aircraft Eng. and Aerospace Technology, 2001, **73**, pp. 465-471.
9. Ursu, I., et al., *Switching neuro-fuzzy control with antisaturating logic. Experimental results for hydrostatic servoactuators*, Proceedings of the Romanian Academy, Series A, Mathematics, Physics, Technical Sciences, Information Science, 2011, **12**, 3, 231-238.
10. Nilsson, H., et al. *Equivalent temperature and thermal sensation - Comparison with subjective responses*. in *Comfort in the automotive industry- Recent development and achievements*. 1997. Bologna, Italy.
11. ISO, *Ergonomics of the thermal environment -Evaluation of thermal environments in vehicles Part 2: Determination of Equivalent Temperature*, in *ISO 14505-2:2006*. 2006, ISO.